Available online at www.sciencedirect.com
ScienceDirect
Journal of Nuclear Materials 367–370 (2007) 1516–1521
journal of nuclear materials
www.elsevier.com/locate/jnucmat

Pulsed-laser ablation of co-deposits on JT-60 graphite tile

Youichi Sakawa [a,*], Daisuke Watanabe [b], Takahiro Shibahara [b], Kazuyoshi Sugiyama [c], Tetsuo Tanabe [c]

[a] *Institute of Laser Engineering, Osaka University, Yamadaoka, Suita, Osaka 565-0871, Japan*
[b] *Graduate School of Engineering, Nagoya University, Chikusa-ku, Nagoya, Aichi 464-8603, Japan*
[c] *Interdisciplinary School of Engineering Science, Kyushu University, Fukuoka, Fukuoka 812-8581, Japan*

Abstract

Pulsed laser ablation of the co-deposits on a JT-60 open-divertor tile using the fourth harmonic of a 20 ps-Nd: YAG laser has been investigated. With increasing the laser intensity, three regions, non-ablation region (NAR), weak-ablation region (WAR), and strong-ablation region (SAR) were distinguished. Transition from NAR to WAR and WAR to SAR occurred at the threshold laser intensity for laser ablation and that for strong ionization of carbon atoms, respectively. The ablation accompanied desorption of H_2 and C_2H_2, with minor contribution of other hydrocarbons, while production of H_2O was small. In NAR and WAR the number of the hydrogen desorbed by the laser irradiation was less than that of hydrogen retained in the ablated volume, while in SAR it was much larger, owing to thermal desorption of hydrogen gas from the region surrounding the ablated volume. For the ablative removal of hydrogen isotopes, SAR is more desirable because of higher removal efficiency and less production of hydrocarbons.

1. Introduction

Carbon-based material is one of the candidates for plasma facing materials in ITER because of their superior nature at high heat flux. However, a significant fraction of tritium is expected to be retained in the vacuum vessel as co-deposits with eroded carbon materials. In order to decrease the accidental release of tritium into the environment, it is necessary to remove tritium periodically [1]. Various tritium removal methods have been investigated, for example, high temperature (>1000 K) baking under vacuum, CO_2 pellet blast cleaning, ion- and electron–cyclotron resonance-discharge cleanings, helium glow-discharge cleaning, and so on [1]. Although most of the retained hydrogen isotopes are removed if the wall temperature can be raised over 1000 K, it is difficult to achieve such a high temperature in ITER. Glow-discharge cleaning can remove hydrogen isotopes from a wide area that faces the plasma, but those retained in the plasma-shadow regions are hardly removed.

Laser induced desorption (LID) is one of the methods to remove tritium. In 1997, Skinner et al. have proposed to heat co-deposits by scanning them using a continuous-wave (CW) laser and to remove tritium by thermal desorption [2]. Some advantages of tritium removal using lasers are that it is possible

* Corresponding author. Tel./fax: +81 6 6879 8734.
E-mail address: sakawa-y@ile.osaka-u.ac.jp (Y. Sakawa).

0022-3115/$ - see front matter © 2007 Elsevier B.V. All rights reserved.
doi:10.1016/j.jnucmat.2007.04.014

to remove tritium from plasma-shadow regions, the production of hazardous tritiated water is small, and it is not necessary to introduce gases. Many experiments on the removal of hydrogen isotopes from carbon materials have been conducted using several types of light sources with different wavelength, pulse duration, and intensity [3–20]. See Table 1 for a summary.

When a laser beam is irradiated on carbon materials, many different processes can occur depending on the laser intensity I_L. In the region where I_L is less than the threshold intensity $I_{ablation}$ for ablation or vapourization (non-ablation region; NAR), thermal desorption of hydrogen isotopes occurs [3,5,6,9,11,13,17]. When I_L is larger than $I_{ablation}$ (ablation region; AR), sublimation of both carbon materials and hydrogen isotopes occurs, and ablative removal starts [3,7,8,10,12,14–16,18–20]. When pulsed lasers are used, since thermal desorption in NAR is not effective, AR is usually used. When I_L is increased further, ionization of carbon materials due to inverse bremsstrahlung (IB) absorption and multi-photon ionization (MPI) occurs at another threshold laser intensity I_{ionize} [19–21]. When a visible or UV laser is used, I_{ionize} can be explained by using a model that includes both IB and MPI [22]. We refer to the region at $I_{ablation} < I_L < I_{ionize}$ as the 'weak-ablation region' (WAR), and that at $I_L > I_{ionize}$ as the 'strong-ablation region' (SAR) [19,20].

We have studied hydrogen release behavior from a hydrogen-saturated graphite target, in which 10 keV-H^+ ions or 8 keV-D^+ ions are implanted, using a pulsed ArF excimer laser (193 nm) [18,19] or the fourth harmonic (266 nm) of a Nd:YAG laser [19,20]. When the Nd:YAG laser is used, since the pulse duration is 20 ps, experiments in a wide laser-intensity region, including NAR, WAR, and SAR, can be achieved. In this paper, we report the LID properties of co-deposits on a JT-60 graphite tile using the ps-266 nm laser. Shu et al. have used an ns-ArF excimer laser (193 nm, 25 ns, $I_L < 3 \times 10^8$ W/cm^2) in NAR and WAR to remove hydrogen from the co-deposits on JT-60 graphite tiles [10,12]. We investigate the variation of LID behavior over the laser-intensity region of more than two-orders of magnitude, including NAR, WAR, and SAR mainly by varying the laser-spot size. The optimum laser intensity for the removal of hydrogen isotopes is also discussed.

2. Experimental

Experiments were conducted under the vacuum pressure $<3 \times 10^{-8}$ Torr [20]. The fourth harmonic of a Nd:YAG laser (Continuum Custom PY61C-10, 266 nm, laser energy <3 mJ/pulse, pulse duration ~20 ps, $I_L < 9 \times 10^{11}$ W/cm^2, repetition rate: 10 Hz) was focused on a target surface by a quartz lens of the focal length of 300 mm through a quartz window with a normal direction to the target. Emitted ions and desorbed gases were measured by a time-of-flight mass spectrometer (TOFMS) and a quadrupole mass spectrometer (QMS: ULVAC MSQ-150), respectively. Visible-light emission was monitored by a spectrometer (Hamamatsu C7473). QMS was calibrated to give a partial pressure of H_2 gas using a calibrated ionization vacuum gauge. We measured both the mass spectra of desorbed gases (scan range is $m/e = 1 - 80$, scan speed is ~0.5 s/scan) and time evolution of H_2 gas. Laser intensity was varied in most cases by changing the focal-spot size on the target. Thousand shots of the pulsed laser beam were irradiated on the target. After the laser irradiation, laser-spot sizes were measured by scanning electron microscopy (SEM). Ablation depth of the sample was measured by an optical microscope.

One of the JT-60 open-divertor tiles, which were exposed to 1800 hydrogen discharges from June 1988 to October 1988, with the limiter configuration including 300 lower X-point divertor configura-

Table 1
List of experiments on the removal of hydrogen isotopes from carbon materials

Wavelength	References	Pulse duration	References	Carbon materials	References
Ruby laser (694 nm)	[3,4,7,8,16]	CW-1.06 μm	[9,11,13]	H- or D-implanted graphite	[3,4,18–20]
Nd:YAG ω (1.06 μm)	[9,11,13]	CW-Xe lamp	[5,6]	CVD (C_2H_2) CFC	[5,15]
Nd:YAG 2ω (532 nm)	[14]	Few 100 μs ruby laser	[3,8,16]	CFC or graphite tiles in TFTR	[6,9–11,13]
Nd:YAG 4ω (266 nm)	[9,20]	Few 100 μs Xe lamp	[15]	JET	[7,11,13,16]
ArF (193 nm)	[10,12,18,19]	ns laser	[4,10,12,14,17,18]	TEXTOR-94	[8,16,17]
KrF (243 nm)	[17]	ps laser	[7,19,20]	JT-60	[10,12]
Xe lamp (172 nm)	[5,6,15]			TORE-SUPRA	[14]

tions, was used as a sample. Hirohata et al. have revealed that hydrogen was retained homogeneously in the co-deposits of the JT-60 open-divertor tiles with the nearly constant concentration of H/C ~0.03 or 1.4×10^{21} atoms m^{-2} μm^{-1} using thermal desorption spectroscopy [23]. The sample was cut from the inner divertor area with a dimension of about $30\times10\times1$ mm^3. A cross-sectional view of the sample was observed by SEM; the co-deposits uniformly covered the tile with the thickness of about 35–40 μm.

3. Results and discussion

Fig. 1(a) shows the ablation depth per laser shot Δd measured by an optical microscope versus I_L. Logarithmic dependence of Δd on I_L is known as Beer's law, $\Delta d = \alpha^{-1}\ln(I_L/I_{ablation})$, where α is the linear absorption coefficient and $I_{ablation}$ is the threshold laser intensity for ablation [10,12,24]. Due to the roughness of the surface of the co-deposits, nearly 8 μm in depth is observed even for the sample without laser irradiation of 1000 shots. Therefore, we marked lower error bars of 8 nm. A logarithmic fit of Δd gave $\alpha \sim 35$ μm^{-1}, which was more than an order of magnitude larger than that measured by Shu et al. for JT-60 co-deposits using 25 ns–193 nm laser [10,12], and $I_{ablation} \sim 9\times10^9$ W/cm^2. The reason for the discrepancy in α is probably due to the difference in laser wavelength and pulse duration. The region at $I_L < I_{ablation} \sim 9\times10^9$ W/cm^2 is NAR. The co-deposits can be removed within 500 shots of the laser irradiation for $I_L > 10^{11}$ W/cm^2, since the thickness is 35–40 μm.

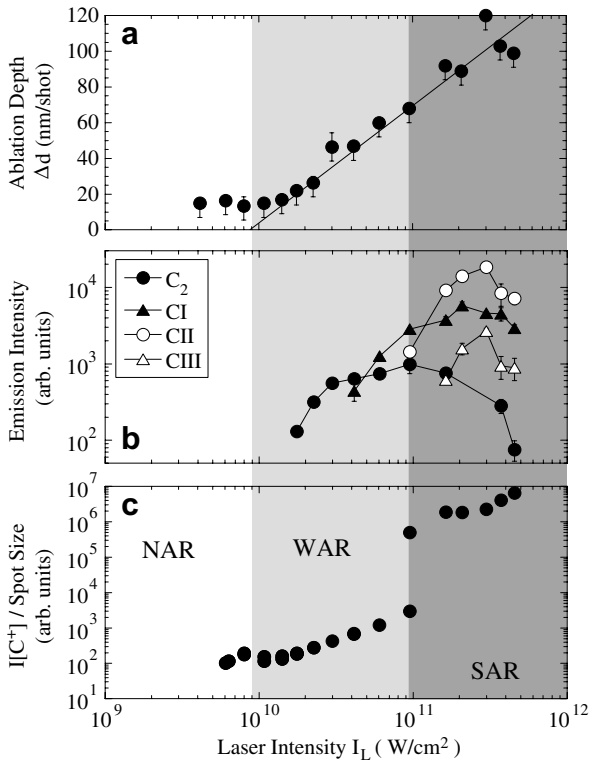

Fig. 1. (a) Ablation depth per laser shot Δd; (b) intensities of optical emission I[C_2] (471.5 nm), I[CI] (909.4 nm), I[CII], (426.7 nm), and I[CIII] (465.1 nm) roughly at the 600th laser shot; and (c) C^+ signal intensity I[C^+] of TOFMS versus laser intensity I_L.

Intensities of the optical emission from C_2 molecules (I[C_2], 471.5 nm), C atoms (I[CI], 909.4 nm), C^+ ions (I[CII], 426.7 nm), and C^{2+} ions (I[CIII], 465.1 nm) roughly at the 600th laser shot versus I_L are displayed in Fig. 1(b). When $I_L < 4\times10^{10}$ W/cm^2, only C_2 Swan band ($d^3\Pi_g - a^3\Pi_u$) emission, for example at 469.7, 471.5, and 516.5 nm, was observed. By increasing I_L, CI, CII, and CIII emission appeared in this order. The intensity of the maximum C^+ signal I[C^+] of TOFMS versus I_L is shown in Fig. 1(c). At the threshold laser intensity of $I_{ionize} \sim 9\times10^{10}$ W/cm^2, I[C^+] increased more than two-orders of magnitude, and I[CII] started to appear, i.e., strong ionization of carbon occurred. Therefore, the region at $I_{ablation} \sim 9\times10^9$ W/cm^2 $< I_L < I_{ionize} \sim 9\times10^{10}$ W/cm^2 is WAR, and that at $I_L > I_{ionize}$ is SAR. Two threshold intensities $I_{ablation}$ and I_{ionize} were nearly identical to those obtained for H^+- or D^+-implanted isotropic graphite, which has nearly an order of magnitude larger H/C ratio than that of JT-60 graphite tile, with the same laser system and irradiation condition [19,20]. TOFMS measurements revealed that, whereas large-size carbon-cluster ions C_n^+ were emitted in WAR, emitted ions were mostly C^+ and C^{2+} in SAR. Similar results have been reported in Refs. [19,20].

Fig. 2(a) displays the mass distribution of residual gases in the vacuum chamber measured by QMS before the laser irradiation. QMS signals were dominated mostly by $m/e = 18$ (H_2O), and a small amount of 2(H_2), 17 (OH), 28 (CO) and 44 (CO_2) signals were observed. By subtracting the intensities of the residual gases (Fig. 2(a)) from that in the first mass scan after the laser shot (Fig. 2(b)), the mass spectrum of the desorbed gases by the laser irradiation at $I_L = 3.7\times10^{11}$ W/cm^2 was derived as shown in Fig. 2(c). Since it takes ~0.5 s to complete a mass

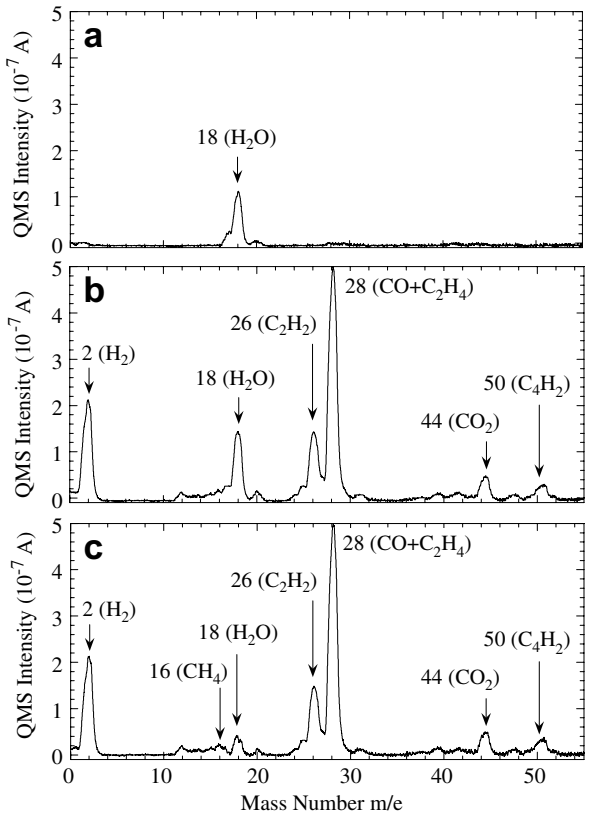

Fig. 2. Mass distribution of the desorbed gases (a) before and (b) after the laser shot. (c) Signal intensities desorbed by the laser irradiation, obtained by subtracting (a) from (b). $I_L = 4.6 \times 10^{11}$ W/cm^2 in SAR.

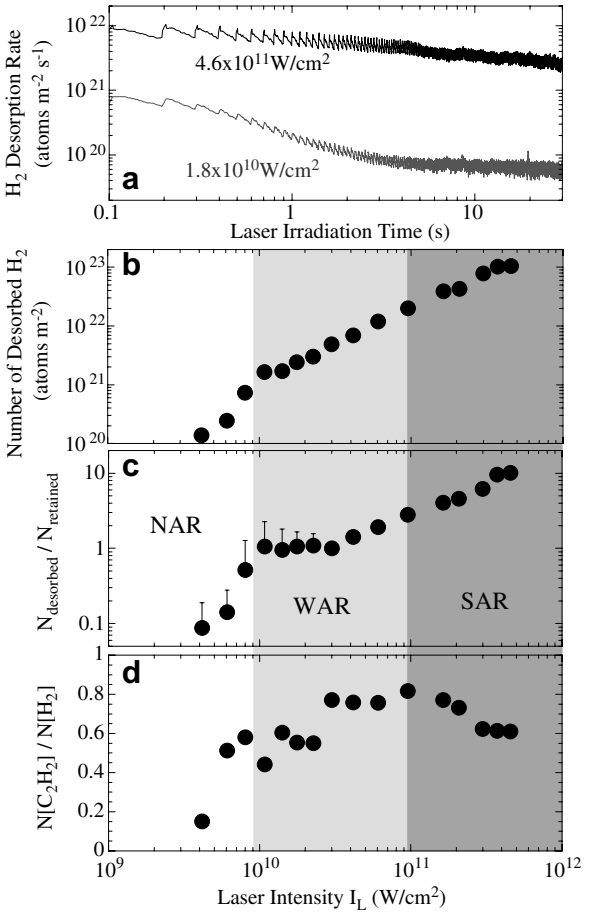

Fig. 3. (a) Time evolution of H_2 desorption rate per laser-spot size at $I_L = 4.6 \times 10^{11}$ W/cm^2 (in SAR) and 1.8×10^{10} W/cm^2 (in WAR). (b) Number of the H_2 molecules desorbed during 300 shots of laser irradiation ($N_{desorbed}$) per laser-spot size, (c) the ratio between $N_{desorbed}$ and the number of hydrogen molecules retained in the ablated volume ($N_{desorbed}/N_{retained}$), and (d) the ratio between the number of C_2H_2 and H_2 molecules desorbed during 300 shots of laser irradiation ($N[C_2H_2]/N[H_2]$) versus I_L.

scan, the mass distribution consists of the signals desorbed by the first to, at most, the fifth laser shots. Desorption of chemical species of $m/e = 2$ (H_2), 26 (C_2H_2), and 28 ($CO + C_2H_4$) was significant, whereas only small increases of those with $m/e =$ 12–16 (CH_m), 18 (H_2O), 44 (CO_2) were observed. The chemical species that desorbed by the laser irradiation were nearly independent on I_L. Note that desorption of H_2O was small, because oxygen retained in the tile was very small compared to hydrogen. Hence production of hazardous tritiated water during tritium removal can be small.

Time evolution of H_2 desorption rate divided by a laser-spot size, determined by the QMS H_2 signal intensity I[H_2] and the measured pumping speed, is shown in Fig. 3(a). Succeeding stepwise increases in I[H_2] at every 0.1 s correspond to the desorption of H_2 gas by each laser shot. For the lower I_L, since the amount of the desorbed gas was smaller, the H_2 desorption rate decreased faster in time. Fig. 3(b) displays the number of the H_2 molecules desorbed during 300 shots of laser irradiation ($N_{desorbed}$), which was obtained by integrating the H_2 desorption rate shown in Fig. 3(a) over the initial 30 s. One can note the drastic increase at $I_{ablation} \sim 9 \times 10^9$ W/cm^2.

Fig. 3(c) represents the ratio between the number of the desorbed hydrogen by the laser irradiation of 300 shots and that of hydrogen retained in the ablated volume, $N_{desorbed}/N_{retained}$. The ablated volume was calculated from the measured ablation depth and the laser-spot size, assuming a parabolic radial ablation profile. Hydrogen was retained homogeneously in the co-deposits with the nearly constant concentration of H/C ~ 0.03 or 1.4×10^{21}

atoms m^{-2} μm^{-1}, as mentioned earlier [23]. Error bars appear from the errors in the ablation depth shown in Fig. 1(a). $N_{desorbed}/N_{retained}$ was below 1 in NAR, nearly equal to 1 in WAR, and over 3 in SAR. Since we calculated the number of desorbed hydrogen only as H_2 molecules in Fig. 3(c), if we include that as hydrocarbon molecules, $N_{desorbed}/N_{retained}$ becomes larger than 1 even at WAR. A possible reason for why the amount of the desorbed hydrogen exceeded that retained in the ablated volume is that hydrogen was also released from the region surrounding the ablated volume, owing to the temperature increase caused by the succeeding laser irradiation.

The ratio between the number of C_2H_2 and H_2 molecules desorbed during 300 shots of laser irradiation ($N[C_2H_2]/N[H_2]$) versus I_L is shown in Fig. 3(d). In NAR, both C_2H_2 and H_2 signal intensities decreased below the detection limit before 300 shots. In NAR and WAR, $N[C_2H_2]/N[H_2]$ increased by increasing I_L, while it decreased by increasing I_L in SAR. Since most of the hydrocarbons have large sticking coefficients, they can be easily deposited on the line-of-sight surface of the vacuum vessel. Not only tritiated water vapour, but also tritiated hydrocarbons, are much more hazardous to humans than tritium gas. Therefore, NAR and SAR are more suitable, since a larger amount of the accumulated tritium is removed as tritium gas.

When LID is used for tritium removal, we have two choices; one is thermal desorption and the other is ablative removal. When the thermal desorption method is used in NAR, the thickness of the co-deposits is unchanged with LID and keeps increasing with tokamak discharges. When the ablative removal of tritium is used in AR, co-deposits can be removed until bulk surface of graphite appears, and SAR is more desirable because of larger removal efficiency and less production of tritiated hydrocarbons. Although carbon is simultaneously removed, it would stick or re-deposit somewhere near the ablated area without incorporation of tritium.

4. Summary and conclusions

Pulsed laser ablation of the co-deposits on JT-60 open-divertor tile has been investigated using the fourth harmonic emission (266 nm) of a 20 ps Nd:YAG laser. By increasing I_L, three regions, the non-ablation region (NAR), the weak-ablation region (WAR), and the strong-ablation region (SAR) were distinguished. In WAR, large-size carbon-cluster ions C_n^+ were emitted, and only C_2 Swan band and CI emissions appeared in visible emission spectra. In SAR, where strong ionization of carbon atoms occurred, emitted ions were mostly C^+ and C^{2+}, and optical emission of CII and CIII lines appeared. The ablation accompanied desorption of H_2 and C_2H_2 with minor contributions of other hydrocarbons, while production of H_2O was small. The ratio of the number of the desorbed hydrogen $N_{desorbed}$ by the laser irradiation to that of hydrogen retained, $N_{retained}$, in the ablated volume was below, nearly equal to, and above 1 in NAR, WAR, and SAR, respectively. The reason for $N_{desorbed} > N_{retained}$ in SAR was explained by thermal desorption of hydrogen gas from the region surrounding the ablated volume. For the ablative removal of hydrogen isotopes, SAR is more desirable because of a larger removal efficiency and less production of hydrocarbons.

Acknowledgement

This work has been partly supported by a Grant-in-Aid for Scientific Research by the Ministry of Education, Culture, Sports, Science and Technology of Japan (Grant No. 17206092).

References

[1] G. Federici, R.A. Anderl, P. Andrew, J.N. Brooks, R.A. Causey, J.P. Coad, D. Cowgill, R.P. Doerner, A.A. Haasz, G. Janeschitz, W. Jacob, G.R. Longhurst, R. Nygren, A. Peacock, M.A. Pick, V. Philipps, J. Roth, C.H. Skinner, W.R. Wampler, J. Nucl. Mater. 266–269 (1999) 14.
[2] C.H. Skinner, H. Kugel, D. Mueller, B.L. Doyle, W.R. Wampler, in: Proc. 17th IEEE/NPSS Symposium on Fusion Engineering, San Diego, 1997, IEEE Piscataway, NJ, USA, 1998, p. 321.
[3] K. Tokunaga, H. Yagi, S. Fukuda, T. Muroga, N. Yoshida, J. Nucl. Mater. 212–215 (1994) 1467.
[4] D. Keroack, B. Terreault, J. Nucl. Mater. 231 (1996) 47.
[5] Y. Oya, W. Shu, S. O'hira, T. Hayashi, H. Nakamura, T. Sakai, T. Tadokoro, K. Kobayashi, T. Suzuki, M. Nishi, J. Nucl. Mater. 290–293 (2001) 469.
[6] W.M. Shu, S. Ohira, C.A. Gentile, Y. Oya, H. Nakamura, T. Hayashi, Y. Iwai, Y. Kawamura, S. Konishi, M.F. Nishi, K.M. Young, J. Nucl. Mater. 290–293 (2001) 482.
[7] D.D.R. Summers, M.N.A. Beurskens, J.P. Coad, G. Counsell, W. Fundamenski, G.F. Mattews, M.F. Stamp, J. Nucl. Mater. 290–293 (2001) 496.
[8] A. Huber, M. Mayer, V. Philipps, A. Pospieszczyk, T. Ohgo, M. Rubel, B. Schweer, G. Serginenko, T. Tanabe, Phys. Scripta. T94 (2001) 102.
[9] C.H. Skinner, C.A. Gentile, A. Carpe, G. Guttadora, S. Langish, K.M. Young, W.M. Shu, H. Nakamura, J. Nucl. Mater. 301 (2002) 98.

[10] W.M. Shu, Y. Kawakubo, M.F. Nishi, Appl. Phys. A76 (2003) 421.
[11] C.H. Skinner, N. Bekris, J.P. Coad, C.A. Gentile, M. Glugla, J. Nucl. Mater. 313–316 (2003) 496.
[12] W.M. Shu, Y. Kawakubo, K. Masaki, M.F. Nishi, J. Nucl. Mater. 313–316 (2003) 584.
[13] C.H. Skinner, N. Bekris, J.P. Coad, C.A. Gentile, A. Hassanein, R. Reiswig, S. Willms, Phys. Scripta. T103 (2003) 34.
[14] F. Le Guern, C. Hubert, S. Mousset, E. Gauthier, C. Blanc, P. Wodling, J.M. Weulersse, J. Nucl. Mater. 410–416 (2004) 410.
[15] K.J. Gibson, G.F. Counsell, C. Curran, M.J. Forrest, M.J. Kay, K.G. Watkins, J. Nucl. Mater. 337–339 (2005) 565.
[16] B. Schweer, A. Huber, G. Sergienko, V. Phillips, F. Irrek, H.G. Esser, U. Samm, M. Kempenaars, M. Stamp, C. Gowers, D. Richards, J. Nucl. Mater. 337–339 (2005) 570.
[17] B. Emmoth, S. Khartsev, A. Pisarev, A. Grishin, U. Karlsson, A. Litnovsky, M. Rubel, P. Wienhold, J. Nucl. Mater. 337–339 (2005) 639.
[18] T. Shibahara, Y. Sakawa, T. Tanabe, J. Nucl. Mater. 337–339 (2005) 654.
[19] Y. Sakawa, T. Shibahara, K. Sato, T. Tanabe, J. Plasma Fusion Res. Ser. 7 (2006) 138.
[20] Y. Sakawa, K. Sato, T. Shibahara, T. Tanabe, Fusion Eng. Des. 81 (2006) 381.
[21] E.G. Gamaly, A.V. Rode, B. Luther-Davies, Appl. Phys. A 69 (Suppl.) (1999) S121.
[22] A. Amoruso, R. Bruzzese, N. Spinelli, R. Velotta, J. Phys. B, At. Mol. Opt. Phys. 32 (1999) R131.
[23] Y. Hirohata, T. Shibahara, T. Tanabe, et al., J. Nucl. Mater. 337–339 (2005) 609.
[24] S.R. Cain, F.C. Burns, J. Appl. Phys. 71 (1992) 4107.